

Electronic Supporting Information (ESI)

Sortase-Mediated Site-Specific Conjugation and Radiolabeling of Designed Ankyrin Repeat Proteins for PET

Rachael Fay¹, Imre Törő², Anna-Lena Schinke², Branko Simic,² Jonas V. Schaefer², Birgit Dreier²,
Andreas Plückthun², and Jason P. Holland^{1*}

¹ University of Zurich, Department of Chemistry, Winterthurerstrasse 190, 8057 Zurich, Switzerland

² University of Zurich, Department of Biochemistry, Winterthurerstrasse 190, 8057 Zurich, Switzerland

*** Corresponding Author:**

Prof. Dr Jason P. Holland

Tel: +41.44.63.53.990

E-mail: jason.holland@chem.uzh.ch

Website: www.hollandlab.org

Twitter: @HollandLab_

First author:

Rachael Fay

Email: rfay@ararisbiotech.com

Table of Contents

General information	5
<i>Chemicals.....</i>	5
<i>NMR Spectroscopy.....</i>	5
<i>Mass spectrometry</i>	5
<i>Preparative chromatography.....</i>	5
<i>High-performance liquid chromatography</i>	5
<i>Size-exclusion chromatography</i>	5
<i>SDS-PAGE analysis of proteins</i>	5
Coomassie staining.....	6
<i>Radioactivity</i>	6
Gallium-68	6
Zirconium-89.....	6
<i>Cell culture.....</i>	6
General methods in cell culture.....	6
SK-OV-3 cells	6
BT-474 cells	7
<i>Lindmo cell binding assay protocol</i>	7
<i>Animals and xenograft models.....</i>	7
<i>Small-animal PET imaging.....</i>	8
Chemical synthesis and characterization.....	9
<i>Supplemental Scheme 1: Synthesis of DFO-Gly₃ (compound 1) from DFO mesylate</i>	9
<i>Synthesis of compound 2</i>	9
<i>Supplemental Figure 1: ¹H NMR (MeOD, 500 MHz) spectra of compound 2.....</i>	10
<i>Supplemental Figure 2: ¹³C{¹H} NMR (DMSO, 125 MHz) spectra of compound 2</i>	10
<i>Synthesis of compound 1</i>	11
<i>Supplemental Figure 3: ¹H NMR (MeOD, 400 MHz) spectra of compound 1.....</i>	11
<i>Supplemental Figure 4: ¹³C{¹H} NMR (D₂O, 101 MHz) spectra of compound 1</i>	12
Synthesis of non-radioactive Ga and Zr complexes	13
<i>Synthesis of ^{nat}Ga-1 complex</i>	13
<i>Synthesis of ^{nat}Zr-1⁺ complex</i>	13
Radiolabeling of triglycine probes	14
<i>Radiosynthesis of [⁶⁸Ga]Ga-1</i>	14
<i>Radiosynthesis of [⁸⁹Zr]Zr-1⁺ complex</i>	14
<i>Supplemental Figure 5: Chromatographic data on the complexation of compound 1 with either the natural or radioactive isotopes of (A) gallium or (B) zirconium.....</i>	14

Protein expression and purification.....	15
<i>Cloning, expression, and purification of DARPin G3-sortase tag fusion</i>	<i>15</i>
Supplemental Figure 6: SDS PAGE analysis of G3-DARPin-LPETGG-His₆.....	15
<i>Expression and purification of sortase.....</i>	<i>15</i>
Supplemental Figure 7: SDS PAGE analysis of sortase A.....	16
Sortase A-mediated transpeptidation bioconjugation reactions	17
Western blot analysis of sortase A conjugation reactions	17
Western blot protocol	17
Optimized sortase A conjugation procedure	17
Radiolabeling of DFO-G3-DARPin	18
⁶⁸ Ga-radiolabeling of DFO-G3-DARPin	18
Supplemental Figure 8: Chromatographic data associated with radiolabeling and characterization of [⁶⁸Ga]GaDFO-G3-DARPin. (A) Reaction scheme showing the radiosynthesis of [⁶⁸Ga]GaDFO-G3-DARPin. (B) RadioTLC analysis. (C) RadioSEC analysis.	18
⁸⁹ Zr-radiolabeling of DFO-G3-DARPin	18
Stability studies using [⁸⁹Zr]ZrDFO-G3-DARPin	19
Chelate challenge: Incubation with excess DTPA	19
Supplemental Figure 9: RadioTLCs in DTPA eluent following the RCP of [⁸⁹Zr]ZrDFO-G3-DARPin over time after DTPA addition.	19
Incubation in human serum.....	19
Incubation in formulation buffer.....	19
Supplemental Figure 10. Data associated with stability studies on [⁸⁹Zr]ZrDFO-G3-DARPin. (A) Plot of change in RCP versus time in the presence of excess DTPA. (B) RadioSEC traces following the stability of [⁸⁹Zr]ZrDFO-G3-DARPin in human serum over time. (C) RadioSEC traces following the stability of [⁸⁹Zr]ZrDFO-G3-DARPin in formulation buffer over time.	20
Cellular binding studies in HER2/neu positive cell lines	20
SK-OV-3 cells.....	20
Supplemental Figure 11: In vitro cell binding of the [⁸⁹Zr]ZrDFO-G3-DARPin radiotracer in SK-OV-3 cells. (A) Saturation binding curve. (B) Reciprocal Lindmo plot.	20
BT-474 cells	21
Supplemental Figure 12: In vitro cell binding of the [⁸⁹Zr]ZrDFO-G3-DARPin radiotracer in SK-OV-3 cells. (A) Saturation binding curve. (B) Reciprocal Lindmo plot.	21
Small-animal PET imaging in BT-474 xenografts using [⁸⁹Zr]ZrDFO-G3-DARPin.....	22
Supplemental Figure 13: Coronal and axial PET images recorded in competitively blocked BT-474 models at 1, 4, 20, and 24 h post-administration of [⁸⁹Zr]ZrDFO-G3-DARPin. B = Bladder, K = Kidney, H = Heart, T = Tumor.	22

Supplemental Figure 14: Maximum intensity projection PET images recorded in BT-474 xenografts at 1, 4, 20, and 24 h post-administration of [⁸⁹ Zr]ZrDFO-G3-DARPin. B = Bladder, K = Kidney, H = Heart, T = Tumor.....	22
Supplemental Figure 15: MIP PET images recorded in competitively blocked BT-474 models at 1, 4, 20, and 24 h post-administration of [⁸⁹ Zr]ZrDFO-G3-DARPin. B = Bladder, K = Kidney, H = Heart, T = Tumor..	23
Ex vivo biodistribution studies of [⁸⁹Zr]ZrDFO-G3-DARPin BT-474 xenografts	23
Supplemental Figure 16: Tumor-to-tissue contrast ratios of the [⁸⁹ Zr]ZrDFO-G3-DARPin recorded at 24 h post-administration in mice bearing BT-474 tumors.	23
Supplemental Table 1: Biodistribution data following the administration of [⁸⁹ Zr]ZrDFO-G3-DARPin in the normal group (n = 3), and blocking group (n = 5) in female athymic nude mice bearing s.c. BT-474 xenografts.	24
Supplemental Table 2: Tumor to tissue contrast data following the biodistribution of [⁸⁹ Zr]ZrDFO-G3-DARPin in the normal group (n = 3), and blocking group (n = 5) in female athymic nude mice bearing s.c. BT-474 xenografts.....	25
Effective half-life measurement	26
Supplemental Figure 17: Plot of the effective half-life (t_{eff} / h) of [⁸⁹ Zr]ZrDFO-G3-DARPin in BT-474 tumor bearing mice for the normal group (blue) and blocking group (black).....	26
References.....	26

General information

Chemicals

Unless otherwise stated, all other chemicals were of reagent grade and purchased from SigmaAldrich (St. Louis, MO), Merck (Darmstadt, Germany), Tokyo Chemical Industry (Eschborn, Germany), aber (Karlsruhe, Germany) or CheMatech (Dijon, France). Water ($>18.2 \text{ M}\Omega\cdot\text{cm}$ at 25°C , Puranity TU 3 UV/UF, VWR International, Leuven, Belgium) was used without further purification. Solvents for reactions were of reagent grade, and where necessary, were dried over molecular sieves. Evaporation of the solvents was performed under reduced pressure by using a rotary evaporator (Rotavapor R-300, Büchi Labortechnik AG, Flawil, Switzerland) at the specified temperature and pressure.

NMR Spectroscopy

^1H and ^{13}C NMR spectra were measured in deuterated solvents on a Bruker AV-400 (^1H : 400 MHz, ^{13}C : 100.6 MHz) or a Bruker AV-500 (^1H : 500 MHz, ^{13}C : 125.8 MHz) spectrometer. Chemical shifts (δ) are expressed in parts per million (ppm) relative to the resonance of the residual solvent peaks, for example, with DMSO $\delta_{\text{H}} = 2.50 \text{ ppm}$ and $\delta_{\text{C}} = 39.5 \text{ ppm}$ with respect tetramethylsilane (TMS, δ_{H} and $\delta_{\text{C}} = 0.00 \text{ ppm}$). Coupling constants (J) are reported in Hz. Peak multiplicities are abbreviated as follows: s (singlet), d (doublet), dd (doublet of doublets), t (triplet), q (quartet), m (multiplet), and br (broad).

Mass spectrometry

High-resolution electrospray ionization mass spectra (HR-ESI-MS) were measured by the mass spectrometry service at the Department of Chemistry, University of Zurich.

Preparative chromatography

Column chromatography was performed by using Merck silica gel 60 (63 – 200 μm) with eluents indicated in the experimental section. Standard thin-layer chromatography (TLC) for synthesis employed Merck TLC plates silica gel 60 on an aluminium base with the indicated solvent system. The spots on TLC were visualised either by UV-visible light (254 nm) or by staining with KMnO_4 .

High-performance liquid chromatography

Analytical high-performance liquid chromatography (HPLC) experiments were performed using Hitachi Chromaster Ultra Rs systems fitted with a reverse phase VP 250/4 Nucleodor C18 HTec (4 mm ID x 250 mm, 5 μm) column. For all HPLC chromatograms: solvent A = $18.2 \text{ M}\Omega\cdot\text{cm H}_2\text{O} + 0.1\% \text{ TFA}$ and solvent B = MeOH and the gradient method used was: 0-2 min 95% A 5% B, 2-12 min 5-100% B.

Size-exclusion chromatography

Automated size-exclusion chromatography was performed using a BioRad 650 column (Bio-Rad Laboratories, ENrich SEC 650, 10 mm ID x 300 mm) connected to a Rigol HPLC system (Contrec AG, Dietikon, Switzerland) equipped with a UV/visible detector (absorption measured at 280 nm) as well as a radioactivity detector (FlowStar2 LB 514, Berthold Technologies, Zug, Switzerland). Isocratic elution with phosphate buffered saline (PBS, pH7.4) was used with a flow rate of 1 mL min^{-1} .

SDS-PAGE analysis of proteins

Samples (15-20 μL) were prepared for SDS-PAGE by mixing single proteins or reaction mixtures, with sample buffer (LDS-Buffer for NuPage) and saline (0.9%). The resulting solutions were heated at 80

°C for 10 min. Samples (10-15 µL) including a protein ladder (Spectra™ Multicolor Broad Range Protein Ladder, ThermoFisher Scientific) were applied to a 4-12% Bis-Tris Gel. The gel was run in NuPage Bis-Tris running buffer (ThermoFisher Scientific) at 55 mA for 70 min. The gel was washed with deionized water before the staining or the transfer procedures.

Coomassie staining

Gels were stained with Coomassie (Coomassie Brilliant Blue G-250) until clear bands could be visualized. This was achieved either by incubation at r.t. with rocking or by boiling in Coomassie by aid of microwave heating. The background was destained by using a destain solution (40% MeOH, 10% AcOH in H₂O). Destaining was performed at r.t. until the background was clear of Coomassie stain.

Radioactivity

Gallium-68

For radiolabeling experiments the ⁶⁸Ga stock solution (in ~0.1 M HCl) was typically added as the limiting reagent to an aqueous reaction mixture buffered with NaOAc (approx. 0.2 M, pH4.4). Radioactive reactions were monitored by using instant thin-layer chromatography (iTLC). Glass-fibre iTLC plates impregnated with silica-gel (iTLC-SG, Agilent Technologies) were developed in citrate buffer (1.0 M, pH4.5, >18.2 MΩ·cm H₂O) or MeOH/H₂O, (1:1 v/v) and analyzed on a radioTLC detector (SCAN-RAM, LabLogic Systems Ltd, Sheffield, United Kingdom). Radiochemical conversion (RCC) was determined by integrating the data obtained by the radioTLC plate reader and determining both the percentage of radiolabelled product and 'free' ⁶⁸Ga. Integration and data analysis were performed by using the software Laura version 5.0.4.29 (LabLogic).

Zirconium-89

[⁸⁹Zr][Zr(C₂O₄)₄]⁴⁻(aq.) was obtained as a solution in ~1.0 M oxalic acid from PerkinElmer (Boston, MA, manufactured by the BV Cyclotron VU, Amsterdam, The Netherlands) and was used without further purification. Unless otherwise stated, ⁸⁹Zr labelling reactions were performed at room temperature at pH 7 – 8.5 (neutralized by using aliquots of 1 M Na₂CO₃). Radioactive reactions were monitored by using instant thin-layer chromatography (radioTLC). Glass-fibre iTLC plates impregnated with silica-gel (iTLC-SG, Agilent Technologies) were developed using DTPA (50 mM, pH7.4) and were analyzed on a radioTLC detector (SCAN-RAM, LabLogic Systems Ltd, Sheffield, United Kingdom). Radiochemical conversion (RCC) was determined by integrating the data obtained by the radioTLC plate reader and determining both the percentage of radiolabelled product and 'free' ⁸⁹Zr (R_f = 1.0; present in the analyses as [⁸⁹Zr][Zr(DTPA)]⁻). Integration and data analysis were performed by using the software Laura version 5.0.4.29 (LabLogic).

Cell culture

General methods in cell culture

All cells were cultured at 37 °C in a humidified, 5% CO₂ atmosphere. All cell media was supplemented with fetal bovine serum (FBS, 10% (v/v), ThermoFisher Scientific) and penicillin/streptomycin (P/S, 1% (v/v) of penicillin 10000 U/mL and streptomycin 10 mg/mL).

SK-OV-3 cells

The human ovarian cancer cell line SK-OV-3 (HER2/*neu* positive) was obtained from the American Type Culture Collection [ATCC-HTB-77], Manassas, VA). Cells were cultured in DMEM/F12 (1:1)

(Dulbecco's Modified Eagle Medium, F-12 Nutrient mixture (Ham)) medium containing [+-]-L-glutamine (2.5 mM). Cells were grown by serial passage and were harvested by using trypsin (0.5%).

BT-474 cells

The human ductal cancer cell line BT-474 (HER2/*neu* positive) was obtained from the American Type Culture Collection [ATCC-HTB-20], Manassas, VA). Cells were cultured in DMEM/F12 (1:1) (Dulbecco's Modified Eagle Medium, F-12 Nutrient mixture (Ham), ThermoFisher Scientific, Schlieren, Switzerland) medium containing [+-]-L-glutamine (2.5 mM). Cells were grown by serial passage and were harvested by using trypsin (0.15%). BT-474 cells were pelleted (100 g, 10 min) and resuspended in media after trypsinization.

Lindmo cell binding assay protocol

Immunoreactivity was determined by using a procedure adapted from Lindmo and coworkers.(1) Cells were harvested and a concentration series of six 1:2 dilutions of cells (in triplicate) was prepared in appropriate cell media. The purified radiotracer was added to each cell concentration in the stated quantities. To determine the extent of non-specific binding, a fourth concentration series of the highest three concentrations of cells was prepared and a specified quantity of non-radiolabeled sample was added to the cell suspension 30 min before the addition of the radiotracer as a blocking agent. Three samples of the same specified quantity of radiotracer were also prepared to serve as standards for total activity added to each sample. To ensure that the cells remained in suspension, they were shaken at 800 rpm at 37 °C in a thermomixer. Cell assays were incubated for 1 h. Then the cells were pelleted by centrifugation (2000 rpm, 4 °C, 4 min), the media was discarded, and the cells were resuspended and washed twice with ice-cold PBS (2 x 1 mL) with re-pelleting and removal of PBS between each wash. Cell-associated radioactivity of the washed pellet was measured by using a gamma counter. The immunoreactive fraction was determined by fitting the saturation binding curve and by transformation of the data to generate the reciprocal Lindmo plot. Data were analyzed by using the GraphPad Prism software.

Animals and xenograft models

All experiments involving mice were conducted in accordance with an animal experimentation license approved by the Zurich Canton Veterinary Office, Switzerland (Jason P. Holland). Experimental procedures also complied with guidelines issued in the *Guide for the Care and Use of Laboratory Animals*.(2) Female athymic nude mice (CrI:NU(NCr)-*Foxn1*^{nu}, 24 – 30 g, 6 – 8 weeks old) were obtained from Charles River Laboratories Inc. (Freiburg im Breisgau, Germany), and were allowed to acclimatize at the University of Zurich Laboratory Animal Services Center vivarium for at least 1 week prior to implanting tumor cells. Mice were provided with food and water *ad libitum*. Tumors were induced on the right shoulder or flank by sub-cutaneous (s.c.) injection of BT-474 cells (10 x 10⁶). The cells were injected in a 1:1 mixture (v/v, 150 µL) of matrigel (Corning® Matrigel® Basement Membrane Matrix, obtained from VWR International) and cell media (DMEM F12 + P/S + FBS).(3) Tumors were monitored over 4.5 weeks and grew to a volume of 25.61 ± 14.40 mm³ (*n* = 8). Tumor volume (*V* / mm³) was estimated by external Vernier caliper measurements of the longest axis, *a* / mm, and the axis perpendicular to the longest axis, *b* / mm. The tumours were assumed to be spheroidal and the volume was calculated in accordance with Equation 1.

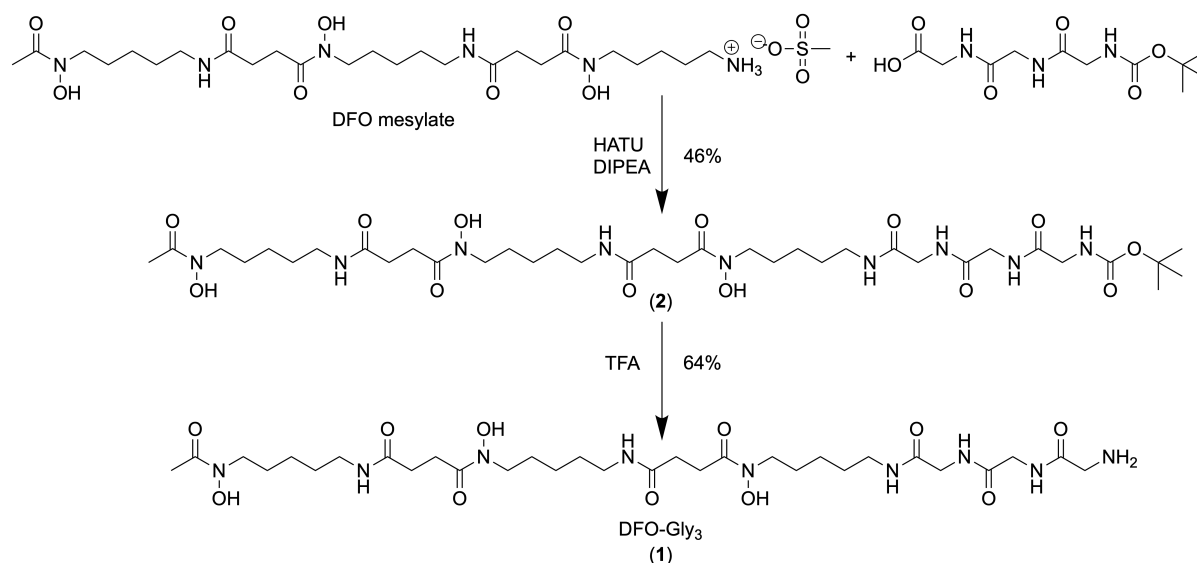
$$V = \frac{4\pi}{3} \cdot \left(\frac{a}{2}\right)^2 \cdot \left(\frac{b}{2}\right) \quad (\text{Equation 1})$$

Small-animal PET imaging

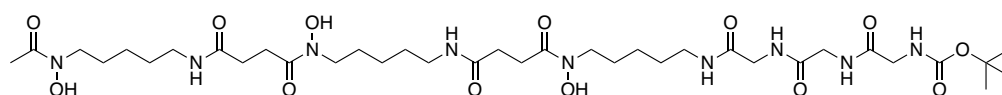
During image acquisition, the respiration rate of the animal was monitored *via* live video feed and anesthesia was maintained by an experienced animal experimenter by controlling the isoflurane dose between 1.5 – 2.0%. List-mode data were acquired for 10 min. by using a γ -ray energy window of 150 – 650 keV, and a coincidence timing window of 20 ns. Images were reconstructed by iterative ordered subset maximum expectation (OSEM; 60 iterations) protocols. Image data were normalized to correct for non-uniformity of response of the PET, attenuation, random events, dead-time count losses, positron branching ratio, and physical decay to the time of injection, but no scatter or partial-volume averaging correction was applied. An empirically determined system calibration factor (in units of [Bq/voxel]/[MBq/g] or [Bq/cm³]/[MBq/g]) for mice was used to convert voxel count rates to activity concentrations. The resulting image data were normalized to the administered activity to parameterize images in terms of %ID/cm³ (equivalent to units of %ID/g assuming a tissue density of unity). Images were analyzed by using VivoQuantTM 3.5 patch 2 software (InviCRO, Boston, MA). For image quantification, 3-dimensional volumes-of-interest (VOIs) were drawn manually to determine the maximum and mean accumulation of radioactivity (in units of %ID/cm³ and decay corrected to the time of injection) in various tissues.

Chemical synthesis and characterization

Supplemental Scheme 1: Synthesis of DFO-Gly₃ (compound 1) from DFO mesylate



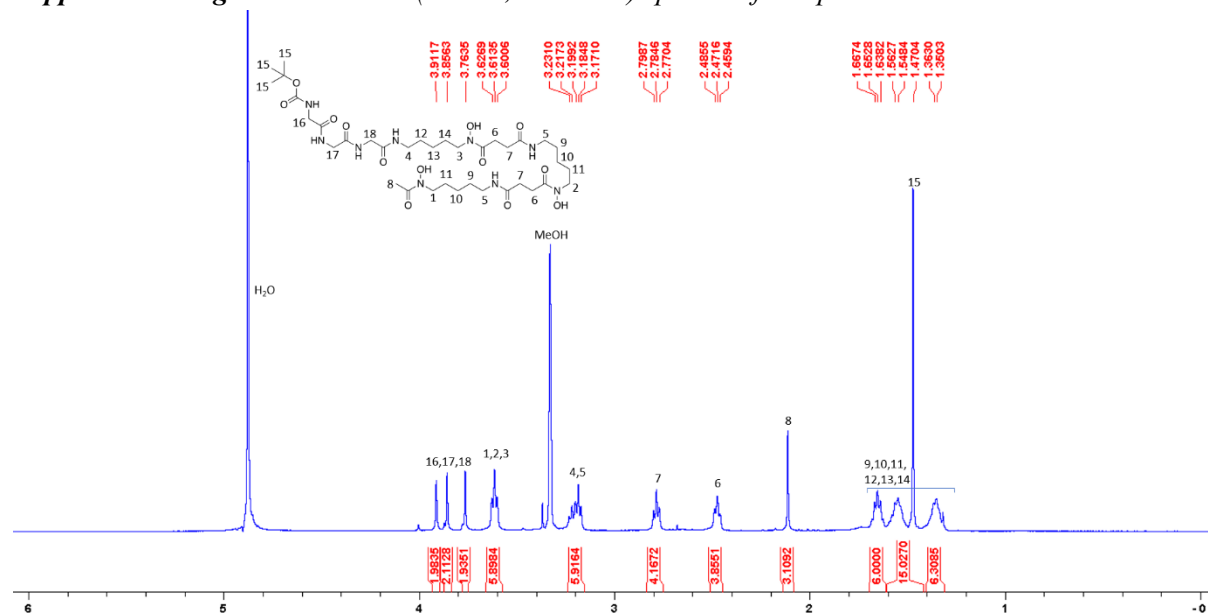
Synthesis of compound 2



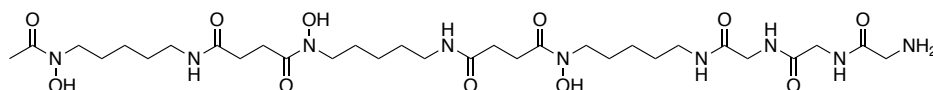
DFO mesylate (1300 mg, 0.46 mmol) was suspended in DMF (6 mL), Boc-Gly₃-OH (171 mg, 0.60 mmol) and HATU (348 mg, 0.92 mmol) and DIPEA (0.18 mL, 1.03 mmol) were added and the solution was stirred at r.t. for 48 h. Unreacted DFO was removed by precipitation from DMF (centrifuge 4000 rpm, 5 min). The remaining DMF solution was concentrated, and the white solid was dissolved in water (25 mL). The aqueous phase was washed with DCM (3 × 20 mL). The aqueous layer was concentrated, and the crude solid was washed with DCM (5 mL) and acetone (3 × 3 mL, then 2 mL, then 1 mL) to yield compound 2 (171 mg, 0.20 mmol, 46%) as a white solid.

¹H NMR (MeOD, 500 MHz): δ 3.89 (s, 2H), 3.84 (s, 2H), 3.75 (s, 2H), 3.60 (t, J = 7.0 Hz, 6H), 3.23 – 3.12 (m, 6H), 2.76 (t, J = 7.3 Hz, 4H), 2.45 (t, J = 7.3 Hz, 4H), 2.09 (s, 3H), 1.68 – 1.59 (m, 6H), 1.58 – 1.48 (m, 6H), 1.45 (s, 9H), 1.40 – 1.28 (m, 6H). ¹³C{¹H} NMR (DMSO, 125 MHz): δ 171.96, 171.28, 170.12, 169.96, 169.06, 168.36, 155.86, 78.16, 47.07, 46.77, 43.34, 42.17, 41.97, 38.41, 29.88, 28.81, 28.74, 28.17, 27.55, 26.02, 23.49, 23.43, 20.35. HRMS (ESI⁺): Calcd for C₃₆H₆₅N₉O₁₃Na, [M + Na]⁺, 854.45941, found 854.45911.

Supplemental Figure 1: ^1H NMR (MeOD, 500 MHz) spectra of compound **2**



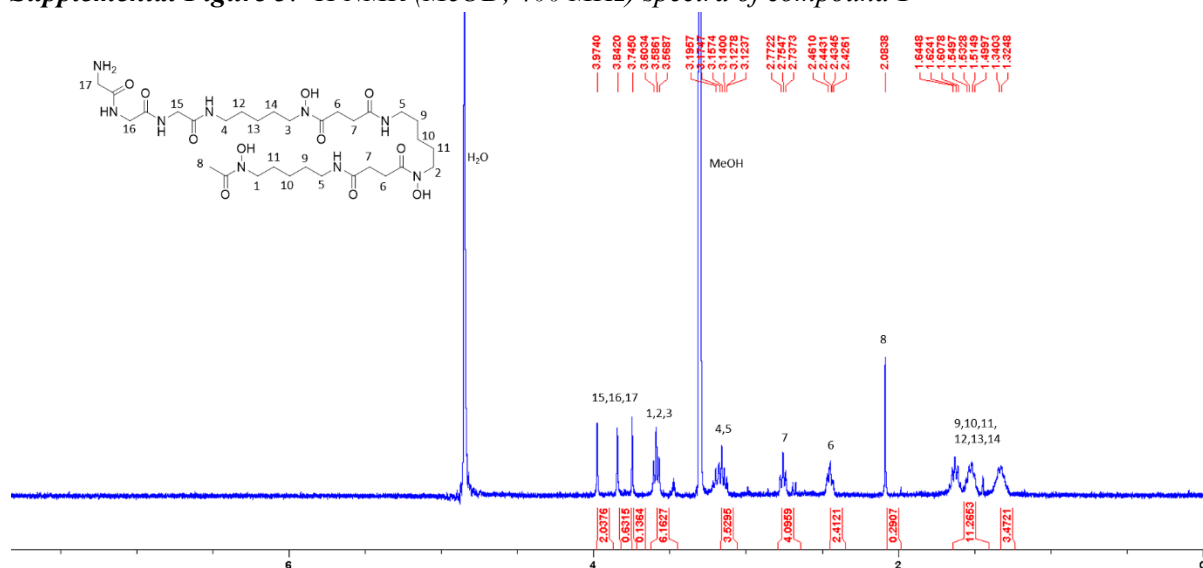
Synthesis of compound 1



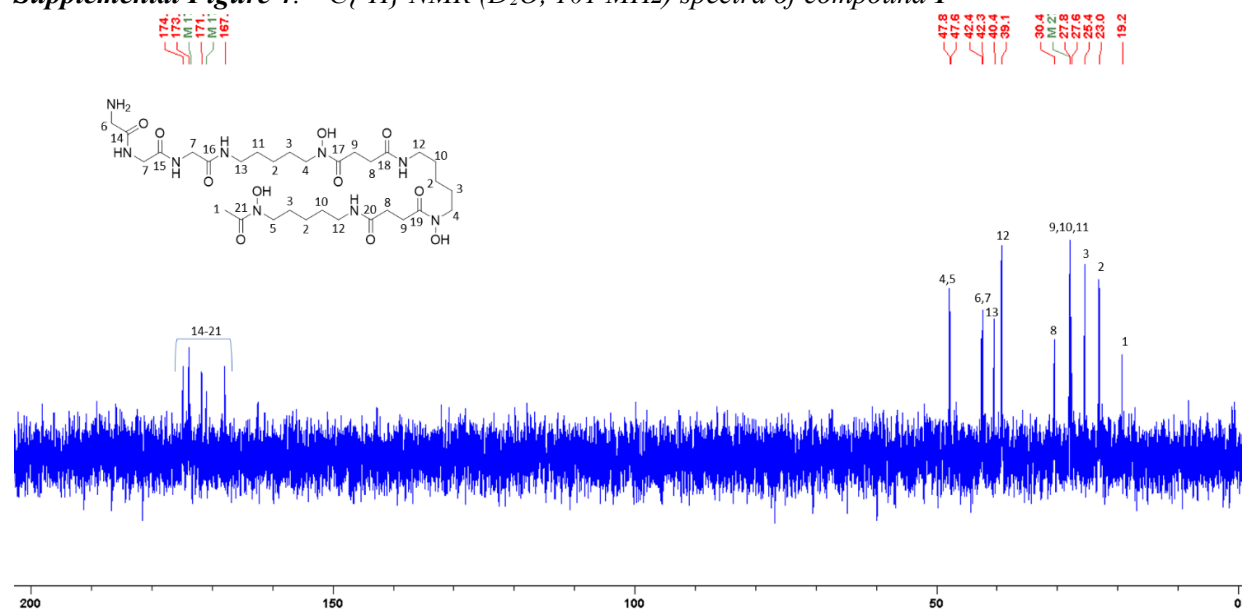
Compound **2** (20 mg, 24.0 μmol) was dissolved in TFA (1 mL) and stirred at r.t. for 1 h. The solution was then precipitated into cold ether (5 mL) and the solid was collected by centrifugation (4000 rpm, 5 min). The collected off white solid was washed with ether (3 mL). The white solid was then purified by semi-preparative HPLC (65% water + 0.1% TFA: 35% MeOH isocratic gradient). The desired compound elutes with a R_t of 20 min. The product fractions were concentrated and lyophilized to yield compound **1** as a white lyophilized solid (11 mg, 15.0 μmol , 64%).

^1H NMR* (MeOD, 400 MHz): δ 3.98 (s, 2H), 3.85 (s, 2H), 3.75 (s, 2H), 3.59 (t, J = 6.7 Hz, 6H), 3.22 – 3.14 (m, 6H), 2.76 (t, J = 7.1 Hz, 4H), 2.45 (t, J = 7.1 Hz, 4H), 2.09 (s, 3H), 1.68 – 1.59 (m, 5H), 1.57 – 1.50 (m, 6H), 1.39 – 1.28 (m, 7H). **^{13}C NMR**** (D_2O , 101 MHz): δ 174.79, 173.81, 173.59, 171.68, 170.95, 167.83, 47.84, 47.68, 42.46, 42.32, 40.41, 39.17, 30.43, 27.86, 27.62, 25.41, 23.02, 19.23) * ^1H NMR in MeOD a singlet was observed for CH_3 , whereas in D_2O two singlets assigned to rotamers were observed. ** ^{13}C NMR was performed in D_2O because the compound is more soluble in water. **HRMS** (ESI^+): Calcd for $\text{C}_{31}\text{H}_{58}\text{N}_9\text{O}_{11}$ $[\text{M}+\text{H}]^+$, 732.42503, found 732.42499. **Analytical HPLC** R_t = 8.47 min.

Supplemental Figure 3: ^1H NMR (MeOD, 400 MHz) spectra of compound 1

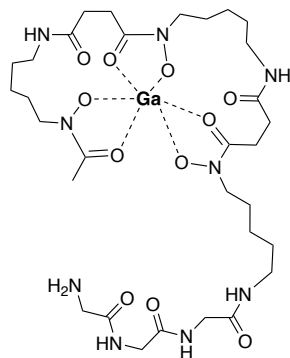


Supplemental Figure 4: $^{13}\text{C}\{^1\text{H}\}$ NMR (D_2O , 101 MHz) spectra of compound **1**



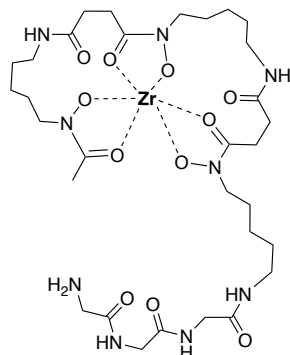
Synthesis of non-radioactive Ga and Zr complexes

Synthesis of $^{nat}\text{Ga-1}$ complex



Compound **1** (0.9 mg, 1.23 μmol) was dissolved in water (500 μL). $\text{Ga}(\text{NO}_3)_3 \cdot \text{H}_2\text{O}$ (0.67 mg, 2.46 μmol) in H_2O (80 μL) was added. After stirring the reaction for 2 h at r.t. The reaction was analyzed by analytical HPLC to show a new peak ($R_t = 7.21$ min, Method A). The reaction was purified by semi-preparative HPLC (Method: 0 – 6 min 5% MeOH, 6 – 40 min 5 – 100% MeOH, 40 – 45 min 100% MeOH). The desired product eluted at 25.6 min. The product was lyophilized to yield $^{nat}\text{Ga-1}$ (0.4 mg, 0.49 μmol , 41%) as a fluffy white lyophilized solid. **HRMS** (ESI $^+$): Calcd for $\text{C}_{31}\text{H}_{54}\text{N}_9\text{O}_{11}\text{GaNa}$, $[\text{M}+\text{Na}]^+$, 820.30907, found 820.30789. **Analytical HPLC** $R_t = 7.21$ min.

Synthesis of $^{nat}\text{Zr-1}^+$ complex



An aqueous solution of compound **1** (100 μL , 1 mg mL^{-1} , 137 nmol) was incubated with $\text{Zr}(\text{acac})_4$ (6.3 μL , 24 mM in MeOH, 151 nmol) at 80 $^\circ\text{C}$ for 1 h. HPLC analysis indicated full conversion to a more polar product. **Analytical HPLC** $R_t = 6.90$ min. **HRMS** (ESI $^+$): Calcd for $\text{C}_{31}\text{H}_{55}\text{N}_9\text{O}_{11}\text{Zr}$, $[\text{M}+\text{H}]^+$, 819.30626, found 819.30469.

Radiolabeling of triglycine probes

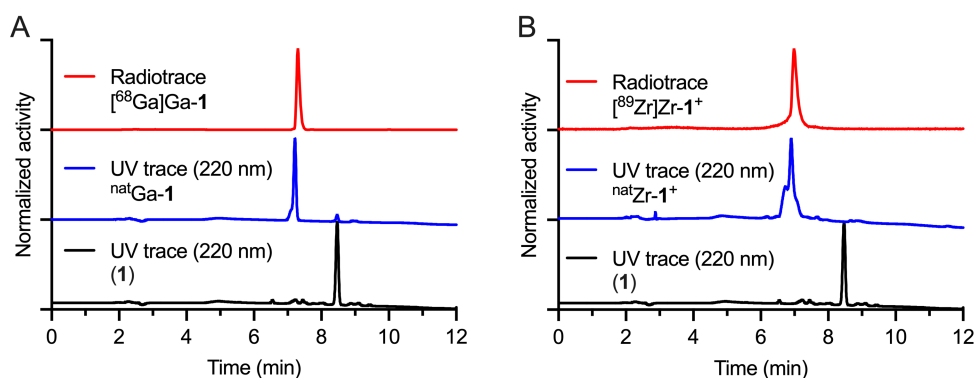
Radiosynthesis of [^{68}Ga]Ga-**1**

An aliquot of compound **1** in water was radiolabeled by adding an aliquot of [^{68}Ga][Ga(H₂O)₆]Cl₃ in sodium acetate buffer at pH 4.0 – 4.5. The resultant [^{68}Ga]Ga-**1** complex gave a single peak in the radioHPLC which coincided with the UV trace of $^{\text{nat}}\text{Ga}$ -**1**. **Analytical HPLC** R_t = 7.30 min.

Radiosynthesis of [^{89}Zr]Zr-**1**⁺ complex

An aliquot of compound **1** in water was radiolabelled by adding an aliquot of [^{89}Zr][Zr(C₂O₄)₄]⁴⁻ at pH 7.5 – 8.0. The resultant [^{89}Zr]Zr-**1**⁺ complex gave a single peak in the radioHPLC which coincided with the UV trace of $^{\text{nat}}\text{Zr}$ -**1**⁺. **Analytical HPLC** R_t = 6.98 min.

Supplemental Figure 5: Chromatographic data on the complexation of compound **1** with either the natural or radioactive isotopes of (A) gallium or (B) zirconium.

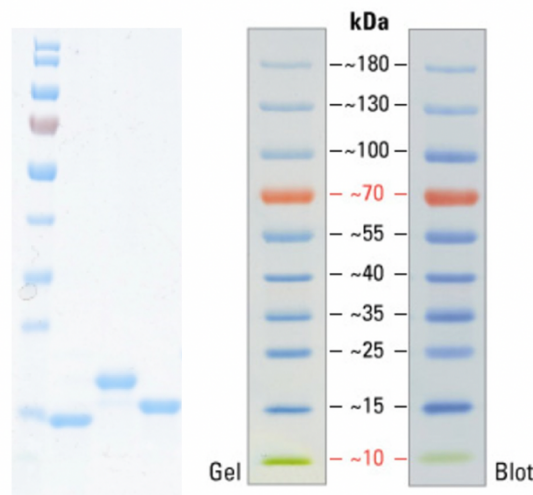


Note: In each plot, the UV trace of the desmetalated ligand (**1**) is shown in black, the UV trace of the non-radioactive metal complex is shown in blue, and the radiotracer of the corresponding radioactive metal ion complex is shown in red.

Protein expression and purification

Cloning, expression, and purification of DARPin G3-sortase tag fusion

The cDNA encoding for DARPin G3 was cloned into the *E. coli* expression plasmid pQiq_K_MRmyc_6His_DARPin_GGGS_LPETGG_6His under the control of a T5/lac promoter.(4,5) Expression was performed using *E. coli* strain BL21Gold in 2YT media (400 mL) supplemented with kanamycin (30 µg/mL) and 1% glucose. Briefly, expression was induced with 0.5 mM IPTG at OD₆₀₀ of 0.9-1. After 4 h at 240 rpm and 37 °C the cells were harvested by centrifugation for 15 min, 4 °C at 5000 g. The pellet was resuspended in ice-cold HBS400 solution (40 mL, 20 mM HEPES pH 7.5, 400 mM NaCl) supplemented with 10 mM MgSO₄, 1 mM CaCl₂, 0.4 µL Pierce™ universal nuclease and protease inhibitors. The cells were lysed using sonication and the lysate cleared by centrifugation for 45 min, 4 °C at 15000 g. The DARPin was purified using a Ni-NTA Superflow column with a CV of 2 mL. Loading was performed in HBS400-W (HBS400, 10% glycerol and 20 mM imidazole). Removal of unbound protein was performed using 40 CV of HBS400-W and 20 CV HBS150 (150 mM NaCl). Elution was performed with 5 mL of HBS150, 300 mM imidazole. The eluate was desalted and the buffer exchanged to HBS150, 5% glycerol using a PD-10 column (GE). DARPins were aliquoted, flash-frozen in liquid nitrogen and stored at -80 °C until further use. For quality control, SDS-PAGE of the G3-DARPin-LPETGG-His₆ construct was performed and is shown in Supplemental Figure 6 (Lane 4).



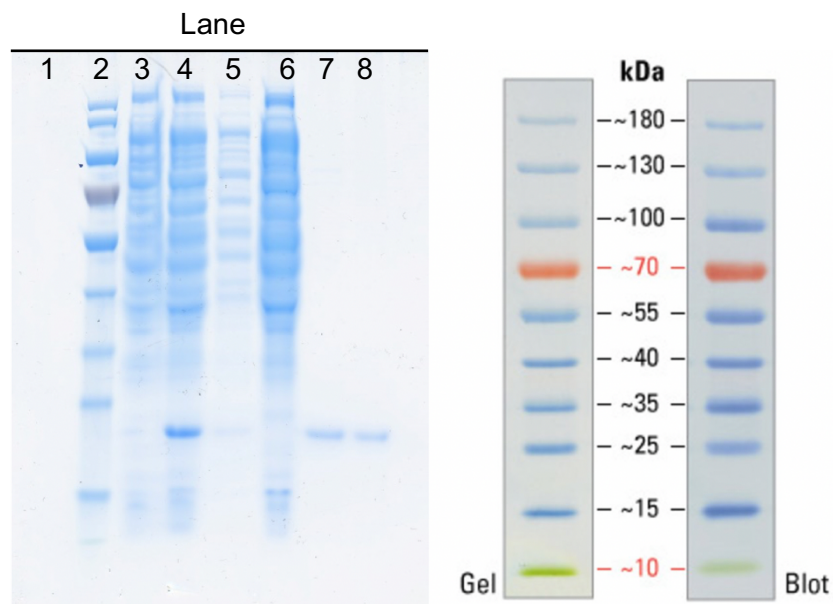
Supplemental Figure 6: SDS PAGE analysis of G3-DARPin-LPETGG-His₆.

Lane 1, molecular weight marker, lane 2, DARPin G3_Cys, lane 3, sortase A enzyme, and lane 4, G3-DARPin-LPETGG-His₆. Protein bands are stained with Coomassie blue.

Expression and purification of sortase

Expression of sortase A was performed using *E. coli* strain BL21Gold in 2YT media (800 mL) supplemented with ampicillin (100 µg/mL) following the standard protocol).(5) Briefly, expression was induced with 0.5 mM IPTG at OD₆₀₀ of 0.8. After 5 h at 240 rpm and 37 °C the cells were harvested by centrifugation for 15 min, 4 °C at 5000 g. The pellet was resuspended in ice-cold HBS400 solution (40 mL, 20 mM HEPES pH=7.5, 400 mM NaCl) supplemented with 10 mM MgSO₄, 1 mM CaCl₂, 0.4 µL Pierce™ universal nuclease and protease inhibitors. The cells were lysed using sonication and the lysate cleared by centrifugation for 45 min, 4 °C at 15000 g. Sortase A was purified using a Ni-NTA Superflow column with a CV of 2 mL. Loading was performed in HBS400-W (HBS400, 10% glycerol and 20 mM imidazole). Removal of unbound protein was performed using 40 CV of HBS400-W and 20 CV HBS150 (150 mM NaCl). Elution was performed with 4 ml of HBS150, 300 mM imidazole. The eluate was dialyzed using the Slide-A-Lyzer Mini Dialysis Devices with a 3.5 kDa MWCO (Thermo Fisher

Scientific). Sortase was aliquoted, flash frozen in liquid nitrogen and stored at -20 °C until further use. For quality control, purification of the sortase construct was performed using SDS-PAGE, and this gel is shown in Supplemental Figure 7 where lane 1 shown the MW marker, and lanes 6 – 7 show the purified sortase enzyme as a single protein band.



Supplemental Figure 7: SDS PAGE analysis of sortase A.

Lane assignments are given in the table below. Protein bands are stained with Coomassie Blue.

Well no.	Sample
1.	Empty
2.	Molecular weight marker
3.	Non-induced control
4.	Induced control
5.	Supernatant (30 μ L contained \sim 4 μ g protein)
6.	Flowthrough (30 μ L undiluted)
7.	Eluate (30 μ L contained \sim 4 μ g protein)
8.	Purified final product (30 μ L contained \sim 4 μ g protein)

Sortase A-mediated transpeptidation bioconjugation reactions

Western blot analysis of sortase A conjugation reactions

Samples were prepared for SDS-PAGE according to the general procedure where 10 μ L aliquots of each reaction were applied to the gel. DARPin samples contained a constant protein mass (2 μ g).

Western blot protocol

Nitrocellulose membrane and filter papers were equilibrated in transfer buffer (Tris-Glycine in MeOH/H₂O). The gel and membrane were packed between filter paper and air bubbles were removed. Transfer was achieved at 65 mA in 60 min by using a Hoefer semi-dry transfer system. The membrane was then washed (PBS/Tween 20, 1% v/v) twice before staining with Ponceau Red. The membrane was cut, de-stained, washed (PBS/Tween) and blocked (5% skim milk powder in PBS/Tween) for 1 h at room temperature.

The anti-His₆ antibody (6x-His Tag Monoclonal Antibody (4E3D10H2/E3) from Invitrogen, 5% skim milk in PBS/Tween solution, 1:10,000 dilution) was added and the membrane was incubated for 1 h at room temperature. The membrane was extensively washed (PBS/Tween) before addition of the secondary antibody (Goat anti-mouse IgG (H+L) (A16066), from Invitrogen, 1:2000 dilution). The membrane was incubated for 30 min at room temperature before washing the membrane three times (PBS/Tween).

WesternBright ECL reagents (Witec AG, Sursee, Switzerland) were added in a 1:1 ratio to the membrane. The membrane was incubated for a few minutes before imaging with Fusion FX7. Images were processed using ImageJ software.

Optimized sortase A conjugation procedure

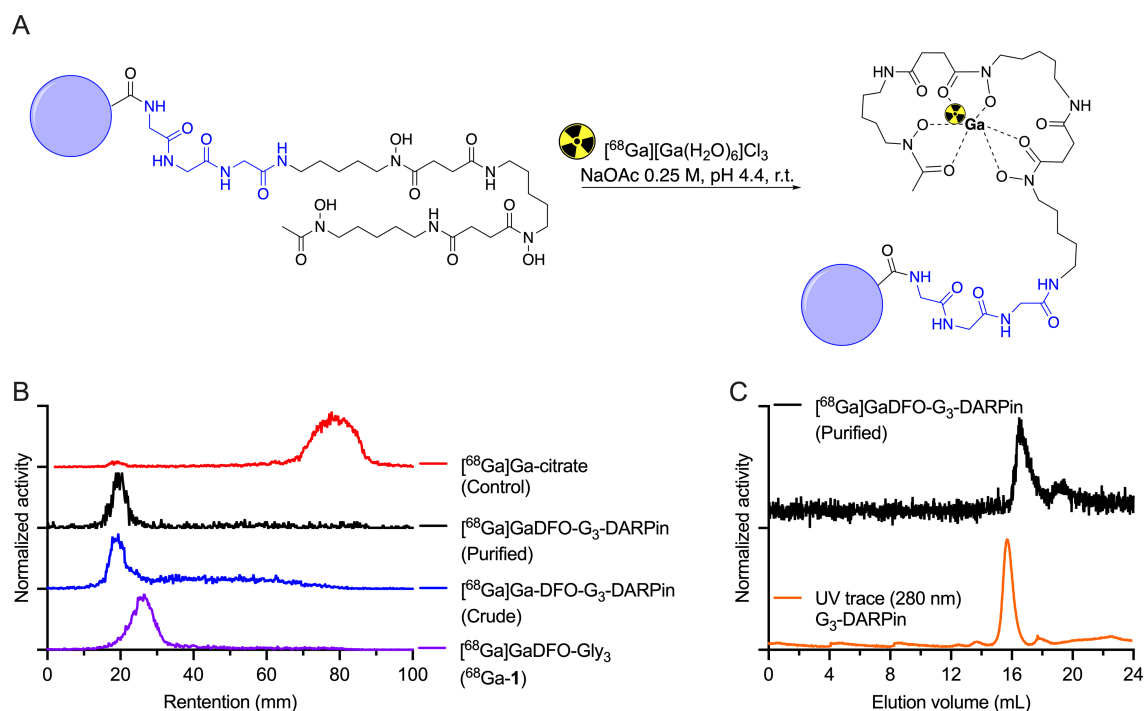
The G3-DARPin-LPETGG-His₆ (38 nmol) was incubated with sortase A (38 nmol) and the triglycine probe (1.9 μ mol, 50 eq.) in 50 mM Tris-HCl, 150 mM NaCl, CaCl₂ (10 mM) at pH 7.9. The reaction was incubated o.n. at 37 °C and 400 rpm. The reaction was then applied to Ni-NTA resin (1 mL) pre-equilibrated with the running buffer (50 mM HEPES, 0.9% NaCl). The flow-through (5 mL) was collected and concentrated by spin-filtration (Amicon Ultra 4, 3 kDa MWCO, 4350 rpm, 30 min). The concentrate was then purified by NAP-10 SEC Chromatography where the dead volume was equal to 0.75 mL and the high molecular weight fraction of 0 – 1.4 mL after the dead volume was collected. The high molecular weight fraction was then concentrated by spin filtration (Amicon Ultra 4, 3 kDa MWCO, 4350 rpm, 30 min) and the concentrate was again purified by Ni-NTA spin filtration (Ni-NTA Spin Kit, Qiagen) to yield the purified conjugate.

Radiolabeling of DFO-G3-DARPin

⁶⁸Ga-radiolabeling of DFO-G3-DARPin

Radiolabeling was performed under standard conditions as shown in the figure below. Starting activities were between 1 – 10 MBq. The radiolabeled protein sample was purified with NAP-5 columns to yield [⁶⁸Ga]GaDFO-G3-DARPin in >85% RCP as determined by radioSEC.

Supplemental Figure 8: Chromatographic data associated with radiolabeling and characterization of [⁶⁸Ga]GaDFO-G3-DARPin. (A) Reaction scheme showing the radiosynthesis of [⁶⁸Ga]GaDFO-G3-DARPin. (B) RadioTLC analysis. (C) RadioSEC analysis.



Note: The purple traces correspond to [⁶⁸Ga]GaDFO-Gly₃ (⁶⁸Ga-1), blue traces correspond to the crude [⁶⁸Ga]Ga-DFO-G3-DARPin, black traces correspond with the purified [⁶⁸Ga]Ga-DFO-G3-DARPin, red traces correspond with the control [⁶⁸Ga][Ga(citrate)₂]³⁻ and in panel C the orange trace indicates the chromatogram of the unmodified G3-DARPin monitored by electronic absorption (UV trace, 280 nm).

⁸⁹Zr-radiolabeling of DFO-G3-DARPin

DFO-G3-DARPin in 50 mM HEPES/0.9% NaCl (75 μ L, 75 μ g) was diluted with H₂O (75 μ L). An aliquot of ⁸⁹Zr (27 μ L, 15.84 MBq) was added to the reaction. After 20 min., radioTLC analysis was performed by spotting an aliquot (~1 μ L) of the crude reaction mixture onto a silica-gel impregnated glass fibre strip and developing with a DTPA eluent (50 mM, pH7.4). RadioTLC analysis showed that 83% of the activity was retained at the baseline. The remaining uncomplexed ⁸⁹Zr was removed by centrifugal spin filtration (4 \times 5 min, 12,000 rpm) using spin filters (Amicon 0.5 mL, 3 kDa MWCO). Between each cycle the protein was re-diluted with 0.1% BSA in PBS). After purification, quality control was performed by using radioTLC. All activity was retained at the baseline. The purified tracer (100 μ L, approx. 22 μ g) was diluted with 0.1% BSA in PBS (450 μ L).

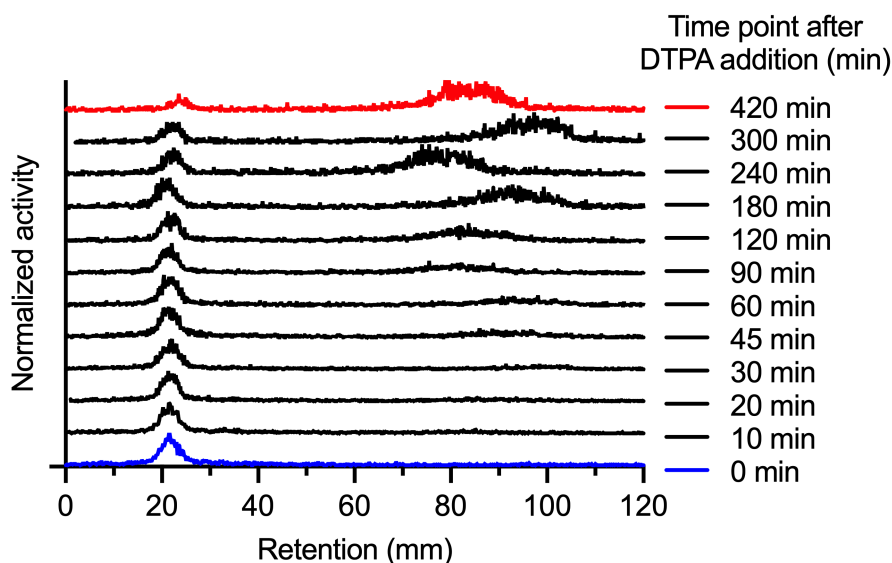
Stability studies using [^{89}Zr]ZrDFO-G3-DARPin

Results from the stability studies performed on [^{89}Zr]ZrDFO-G3-DARPin are summarized below.

Chelate challenge: Incubation with excess DTPA

Purified [^{89}Zr]ZrDFO-G3-DARPin (130 μL , 20 – 25 μg , 1.4–1.7 nmol, 1.439 MBq) was incubated with DTPA (pH 7.4, 50 μL , 50 mM, 2500 nmol, 1470–1785 fold excess) at r.t. and the RCP was monitored by radioTLC at various time intervals over 7 h.

Supplemental Figure 9: RadioTLCs in DTPA eluent following the RCP of [^{89}Zr]ZrDFO-G3-DARPin over time after DTPA addition.



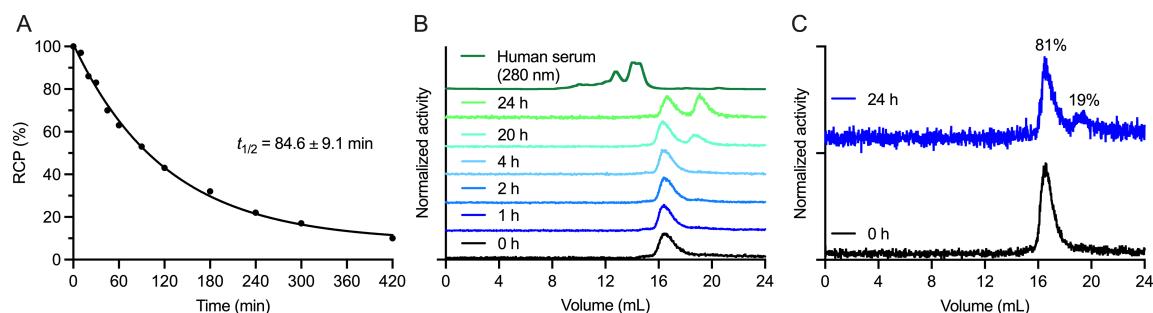
Incubation in human serum

Purified [^{89}Zr]ZrDFO-G3-DARPin (390 μL , 60 – 75 μg , 4.2 – 6.1 nmol, 4.898 MBq) was incubated with human serum (200 μL) at 37 °C. Aliquots of the reaction were analysed by radioSEC at time intervals of 0 h, 1 h, 2 h, 4 h, 20 h and 24 h, as shown in Supplemental Figure 10B.

Incubation in formulation buffer

Purified [^{89}Zr]ZrDFO-G3-DARPin (390 μL , 60 – 75 μg , 4.2 – 6.1 nmol, 4.898 MBq) was incubated in formulation buffer (0.1% BSA in PBS) over 24 h. An aliquot was analyzed by radioSEC at 24 h, as shown in Supplemental Figure 10C.

Supplemental Figure 10. Data associated with stability studies on [^{89}Zr]ZrDFO-G3-DARPin. (A) Plot of change in RCP versus time in the presence of excess DTPA. (B) RadioSEC traces following the stability of [^{89}Zr]ZrDFO-G3-DARPin in human serum over time. (C) RadioSEC traces following the stability of [^{89}Zr]ZrDFO-G3-DARPin in formulation buffer over time.



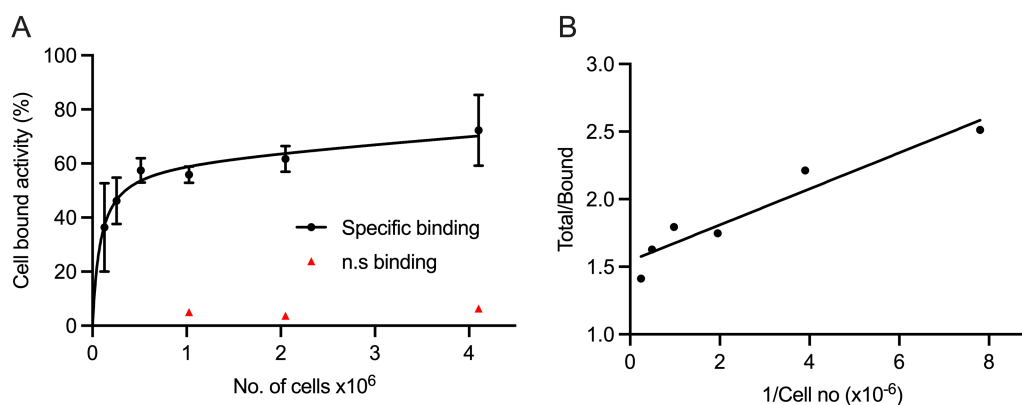
Cellular binding studies in HER2/*neu* positive cell lines

Cellular binding studies were performed to evaluate the specific binding and immunoreactive fraction of [^{89}Zr]ZrDFO-G3-DARPin.

SK-OV-3 cells

[^{89}Zr]ZrDFO-G3-DARPin (5 ng, 0.34 pmol, 6300 Bq) was administered to the normal group. Blocking controls received non-radiolabelled G3-DARPin (5 μg , 0.34 nmol) 30 minutes before the tracer was administered.

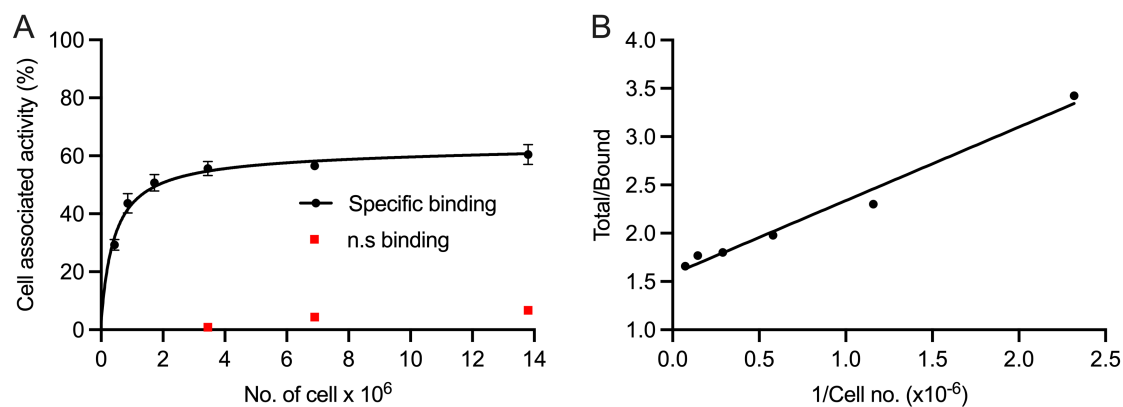
Supplemental Figure 11: *In vitro* cell binding of the [^{89}Zr]ZrDFO-G3-DARPin radiotracer in SK-OV-3 cells. (A) Saturation binding curve. (B) Reciprocal Lindmo plot.



BT-474 cells

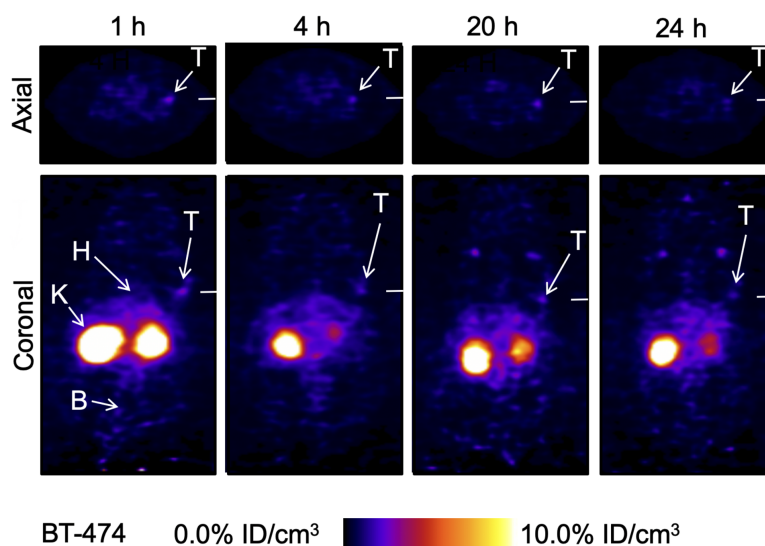
[⁸⁹Zr]ZrDFO-G3-DARPin (4 ng, 0.34 pmol, 2300 Bq) was administered to the normal group. Blocking controls received non-radiolabelled G3-DARPin (5 µg, 0.28 nmol) 30 minutes before the tracer was administered.

Supplemental Figure 12: *In vitro* cell binding of the [⁸⁹Zr]ZrDFO-G3-DARPin radiotracer in SK-OV-3 cells. (A) Saturation binding curve. (B) Reciprocal Lindmo plot.

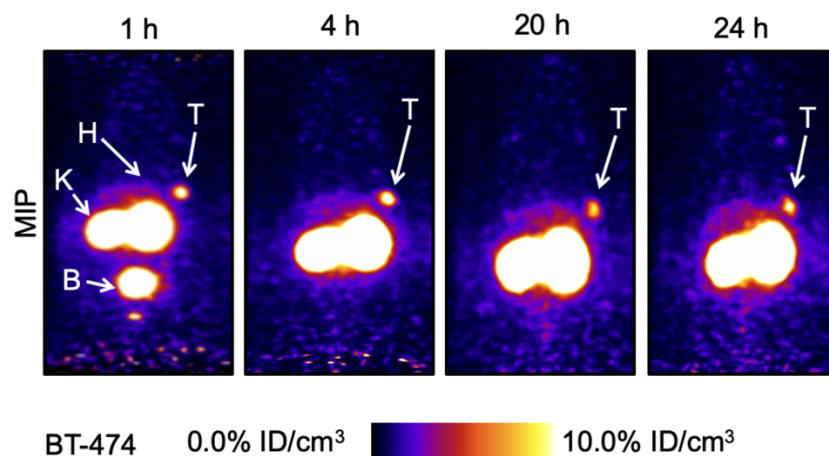


Small-animal PET imaging in BT-474 xenografts using [^{89}Zr]ZrDFO-G3-DARPin

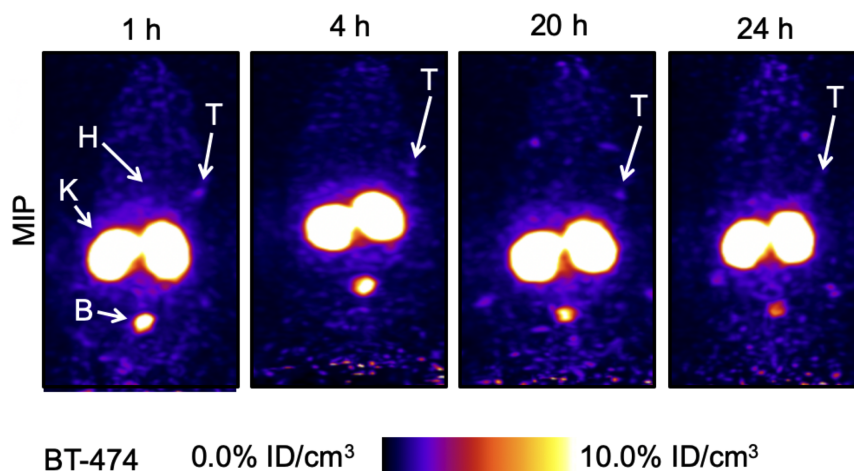
Supplemental Figure 13: Coronal and axial PET images recorded in competitively blocked BT-474 models at 1, 4, 20, and 24 h post-administration of [^{89}Zr]ZrDFO-G3-DARPin. B = Bladder, K = Kidney, H = Heart, T = Tumor.



Supplemental Figure 14: Maximum intensity projection PET images recorded in BT-474 xenografts at 1, 4, 20, and 24 h post-administration of [^{89}Zr]ZrDFO-G3-DARPin. B = Bladder, K = Kidney, H = Heart, T = Tumor.

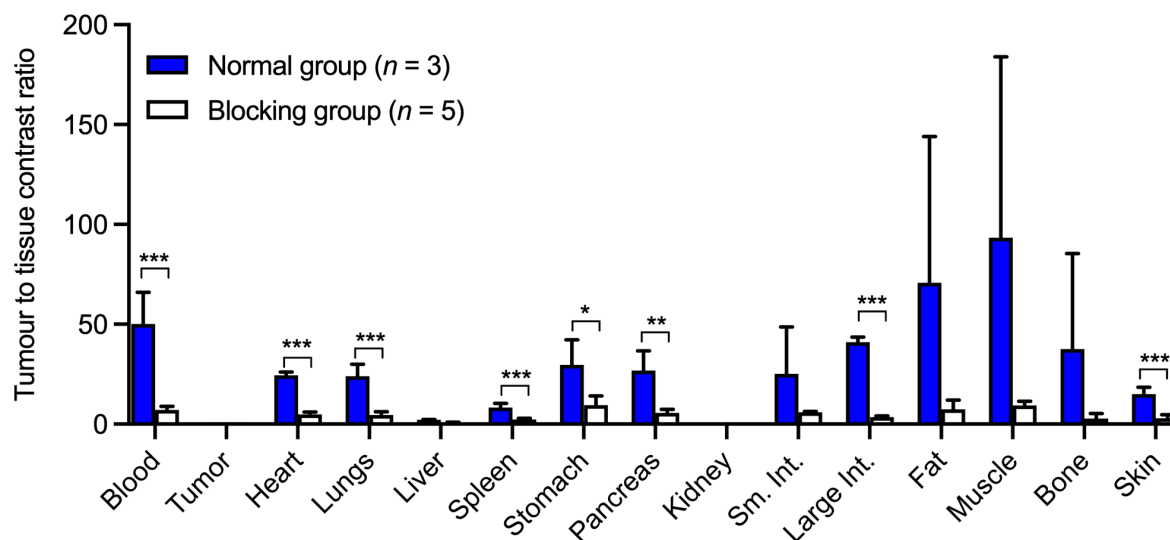


Supplemental Figure 15: MIP PET images recorded in competitively blocked BT-474 models at 1, 4, 20, and 24 h post-administration of [^{89}Zr]ZrDFO-G3-DARPin. B = Bladder, K = Kidney, H = Heart, T = Tumor.



Ex vivo biodistribution studies of [^{89}Zr]ZrDFO-G3-DARPin BT-474 xenografts

Supplemental Figure 16: Tumor-to-tissue contrast ratios of the [^{89}Zr]ZrDFO-G3-DARPin recorded at 24 h post-administration in mice bearing BT-474 tumors.



Supplemental Table 1: Biodistribution data following the administration of [^{89}Zr]ZrDFO-G3-DARPin in the normal group ($n = 3$), and blocking group ($n = 5$) in female athymic nude mice bearing s.c. BT-474 xenografts.

[^{89}Zr]ZrDFO-G3-DARPin (24 h) %ID/g \pm S.D		
Tissue	Normal group ($n = 3$)	Blocking group ($n = 5$)
Blood	0.10 ± 0.04	0.19 ± 0.07
Tumor	4.41 ± 0.67	1.26 ± 0.29
Heart	0.18 ± 0.02	0.26 ± 0.08
Lungs	0.19 ± 0.05	0.29 ± 0.10
Liver	2.04 ± 0.16	1.48 ± 0.15
Spleen	0.54 ± 0.13	0.55 ± 0.14
Stomach	0.17 ± 0.07	0.17 ± 0.10
Pancreas	0.17 ± 0.04	0.26 ± 0.10
Kidney	159.65 ± 14.75	82.77 ± 9.44
Sm. Int.	0.37 ± 0.36	0.21 ± 0.04
Large Int.	0.11 ± 0.01	0.36 ± 0.11
Fat	0.12 ± 0.008	0.19 ± 0.09
Muscle	0.10 ± 0.09	0.13 ± 0.03
Bone	0.30 ± 0.23	0.58 ± 0.26
Skin	0.30 ± 0.05	0.53 ± 0.25

Note: S.D. = 1 standard deviation.

Supplemental Table 2: Tumor to tissue contrast data following the biodistribution of [^{89}Zr]ZrDFO-G3-DARPin in the normal group ($n = 3$), and blocking group ($n = 5$) in female athymic nude mice bearing s.c. BT-474 xenografts.

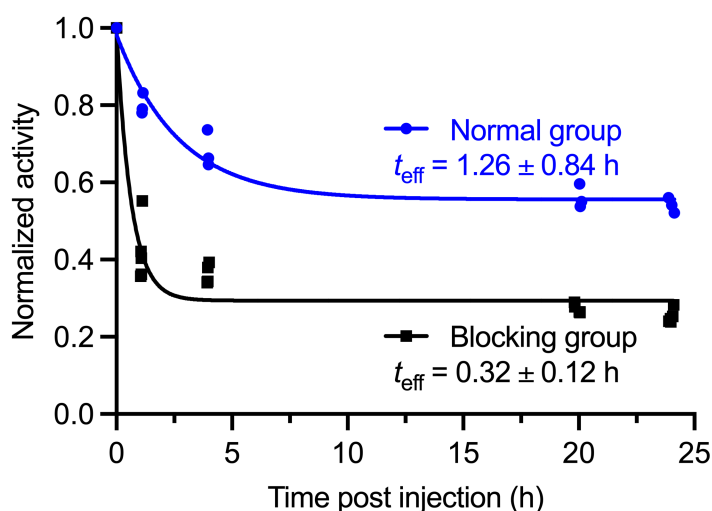
[^{89}Zr]ZrDFO-G3-DARPin (24h), tumor to tissue contrast ratio \pm S.D		
Tissue	Normal group ($n = 3$)	Blocking group ($n = 5$)
Blood	50.12 \pm 15.80	7.09 \pm 1.55
Heart	24.46 \pm 1.70	4.86 \pm 1.03
Lungs	23.96 \pm 6.08	4.52 \pm 1.49
Liver	2.15 \pm 0.18	0.79 \pm 0.12
Spleen	8.37 \pm 1.99	2.31 \pm 0.53
Stomach	29.65 \pm 12.50	9.48 \pm 4.16
Pancreas	26.87 \pm 9.76	5.60 \pm 1.61
Kidney	0.03 \pm 0.00	0.01 \pm 0.01
Sm. Int.	25.12 \pm 23.46	5.88 \pm 0.43
Large Int.	40.96 \pm 2.64	3.54 \pm 0.53
Fat	70.70 \pm 73.32	7.47 \pm 4.06
Muscle	93.28 \pm 90.70	9.34 \pm 1.82
Bone	37.66 \pm 47.73	2.82 \pm 2.23
Skin	14.96 \pm 3.51	2.91 \pm 1.65

Note: S.D. = 1 standard deviation.

Effective half-life measurement

The effective half-life $t_{1/2}(\text{eff})$ of [^{89}Zr]ZrDFO-G3-DARPin was calculated from the measurement of total internal radioactivity over time by using a dose calibrator.

Supplemental Figure 17: Plot of the effective half-life ($t_{\text{eff}} / \text{h}$) of [^{89}Zr]ZrDFO-G3-DARPin in BT-474 tumor bearing mice for the normal group (blue) and blocking group (black).



References

1. Lindmo T, Boven E, Cuttitta F, Fedorko J, Bunn PA. Determination of the immunoreactive function of radiolabeled monoclonal antibodies by linear extrapolation to binding at infinite antigen excess. *J Immunol Methods*. 1984;72:77-89.
2. Institute for Laboratory Animal Research. Guide for the Care and Use of Laboratory Animals: 8th Ed.; 2011.
3. Fridman R, Benton G, Aranoutova I, Kleinman HK, Bonfil RD. Increased initiation and growth of tumor cell lines, cancer stem cells and biopsy material in mice using basement membrane matrix protein (Cultrex or Matrigel) co-injection. *Nat Protoc*. 2012;7:1138-1144.
4. Zahnd C, Wyler E, Schwenk JM, et al. A Designed Ankyrin Repeat Protein Evolved to Picomolar Affinity to Her2. *J Mol Biol*. 2007;369:1015-1028.
5. Andres F, Schwill M, Boersma YL, Plückthun A. High-Throughput Generation of Bispecific Binding Proteins by Sortase A-Mediated Coupling for Direct Functional Screening in Cell Culture. *Mol Cancer Ther*. 2020;19:1080-1088.